The Fourth IEEE RAS/EMBS International Conference
on Biomedical Robotics and Biomechatronics
Roma, Italy. June 24-27, 2012

Simulation of model-based impedance control applied to a biomechatronic exoskeleton with shape memory alloy actuators

André A. M. Araujo, Eduardo A. Tannuri, Arturo Forner-Cordero

Abstract — **This work describes the implementation of impedance control with shape memory alloy (SMA) actuators in a lower limb exoskeleton. Impedance control can be embedded in robotic systems that physically interact with a human user or the environment. In this context, the use of SMA actuators with impedance control to drive the hip joint of a lower limb exoskeleton is assessed. Preliminary simulation results indicate the feasibility of physical implementation of the controller. More precise simulations and prototype testing are being developed before definite conclusions are drawn. System description and modeling is presented, followed by the controller design. Simulations results are presented and discussed.**

I. INTRODUCTION

THIS work proposes an impedance control algorithm to be used in robotic exoskeletons. In this particular case, a lower limb exoskeleton driven by shape memory alloy (SMA) wires is presented. However, the proposed algorithm does not necessarily depend on this type of actuators.

Shape memory alloys are materials which present a property called *shape memory effect*, allowing them to recover a previously defined form by adequate application of heat, even after plastic deformation. Even though there are many alloys that present this property, Ni-Ti (commercially known as *Nitinol*) is the most commonly used.

The first goal of the controller is to provide a zero-force interaction with the user, so no additional effort is required to wear the exoskeleton. The second objective is to provide energy so the user's performance can be augmented with the aid of the device. There is also a third goal, in which the exoskeleton can be used to generate a resistance against the motion of the user increasing the perceived limb impedance. Since SMA wires actuate only in traction and an antagonist mechanism is currently out of scope, the last goal cannot be fully achieved. However, a passive return system based on a spring to implement the antagonist force is being assessed.

The proposed controller can be applied either to increase or decrease the impedance of a human limb. The joint impedance reduction could be useful to assist patients suffering a motor disorder, while increase in impedance could be useful in physical therapy or in sports training.

According to Hogan [1], impedance can be defined as a system which accepts flow (e.g. motion, electrical current) and yields effort (e.g. force, voltage). On the other hand, admittance is defined by a system which accepts effort and yields flow. Since physical systems need to complement each other, then, in this case, the human leg is considered to be an impedance, while the exoskeleton is an admittance.

Aguirre-Ollinger *et al.* [2, 3] have already implemented an assistive exoskeleton for knee joint based on impedance control using a conventional DC motor as actuator. Although the motor has greater power and wider frequency response when compared to SMA wires, it is also heavier. The use of SMA actuators might be interesting in order to keep exoskeletons as lightweight as possible.

Valenzuela *et al.* [4] have designed a biped robot actuated by SMA wires. Because of the slow thermal process involved to contract and relax the wires, instead of using a single wire per actuator, this robot uses a bundle of smaller diameter wires, thus increasing heat exchange area and, consequently, the actuation speed. The robot achieved forces of up to 12N per actuator.

Mathematical models for the SMA nonlinear dynamics have been derived by Ikuta *et al.* [5], Elahinia and Ashrafiuon [6], Grant *et al.* [7], Dutta and Ghorbel [8] and Hoder *et al.* [9]. Romano and Tannuri [10], have constructed a single wire SMA actuator cooled by a thermoelectric element. Using a wire with 0.008" diameter and a Slide Mode controller, they achieved experimentally a cutoff frequency of 0.69 Hz.

Grant and Hayward [11, 12] developed a SMA actuator, comprised of 12 wires working in parallel, and used a two stage relay, force controller to regulate actuation.

The main objective of this work is to assess the feasibility of using an impedance control algorithm to operate a lower limb exoskeleton with SMA actuators.

Only a few works on SMA wires driving exoskeletons have been published so far [13, 14, 15], although there are some publications about robots with this kind of actuator [4, 16, 17, 18, 19]. Nevertheless, Abolfathi [15] described an interesting SMA-actuated exoskeleton for rehabilitation of the hand and discussed why this kind of actuator was not widely used proposing some improvements.

The paper is organized as follows: first, the dynamic model of the system under analysis is presented, comprising the exoskeleton and the SMA actuator; then, the impedance controller algorithm is explained, followed by the SMA actuator controller. Simulation results are presented and

Manuscript received January 31, 2012; revised April 30th, 2012.

André Avelãs Machado de Araujo, Eduardo Aoun Tannuri and Arturo Forner-Cordero are with the Biomechatronics Lab. Department of Mechatronics and Mechanical Systems. Escola Politécnica. University of São Paulo. Brazil. e-mail: andremaraujo@usp.br; eduat@usp.br; aforner@usp.br.

discussed along with future research pathways.

II. System Description

The system studied in this work is a simplified model of the human leg wearing an exoskeleton [3]. For simplicity, only one degree of freedom is considered: the hip flexo-extension (Fig. 1). Both leg and exoskeleton can be modeled as a pendulum. The exoskeleton is acting in parallel with the leg to modify its impedance. The human-exoskeleton parameters are: $J = J_h + J_{exo}$, $B = B_h + B_{exo}$, $M = M_h + M_{exo}$ and $K = K_h + K_{exo}$. Also, $\tau = \tau_h + \tau_{exo}$. Because this is a conceptual work, a reduced scale model will be used (M = 0.5 kg, B = 0.1 kg.m²/s, and d = 0.2 m). There are technological challenges, regarding SMA wire drive and cooling, yet to be addressed in future research before a human scale prototype is designed and constructed, where torques in the order of 10 to 100 N.m are needed [20].

The angle θ ranges from 0 to 40 degrees, with the vertical being 0 degree.

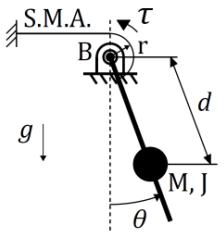

Fig. 1. Diagram representation of the system, where the hip is modeled as a revolute joint and the leg is rigid and modeled as a concentrated mass. The leg and the exoskeleton are rigidly connected and a load cell measures the interaction force between both.

A. Leg and exoskeleton model

The dynamics of the actual system (human leg and exoskeleton) is given by (1):

$$J.\ddot{\theta} + B.\dot{\theta} + M.d.g.sin(\theta) = \tau \qquad (1)$$

where J is the moment of inertia, B is the viscous damping of the joint, M is the mass, d is the distance between center of mass and the joint axis, g is the acceleration of gravity, θ is the angular position of the system, $\dot{\theta}$ is the angular velocity of the system, $\ddot{\theta}$ is the angular acceleration of the system and τ is the torque applied to the system.

The plant model is linearized around θ=0, then, $sin(\theta) \cong \theta$, and the following transfer function (2) can be used, where $K = M.d.g$ is the system stiffness.

$$\frac{\theta(s)}{\tau(s)} = \frac{1}{J.s^2 + B.s + K} \qquad (2)$$

There are several sets of parameters to be considered in the control algorithm. First, the parameters of the human and the exoskeleton, isolated, which will be denoted by the subscripts h and exo, respectively. The sum of these parameters results in those of the actual system. Finally, there are the desired parameters (subscript d), which are used in the control algorithm.

The exoskeleton parameters were considered to be a 10% fraction of those of the human. The desired parameters can be larger, equal or smaller than those of the human. If the desired impedance parameters are chosen to be larger than those of the human, the exoskeleton will act against the motion of the user as a training machine that requires additional effort to move. If the desired impedance is equal to that of the human, the exoskeleton will be transparent to the user. Selecting lower impedance parameters, the exoskeleton will increase the force of the user and improve motion performance.

B. SMA model

The actuator is formed by eight SMA wires working in parallel and cooled by forced convection. The dynamics of the wires are modeled as described by Romano and Tannuri [10]; the torque on each wire is given by (3):

$$\tau_{SMA} = r.[(1-\xi).E_A].\frac{A_t}{l_0}.(0{,}04.l - x) \qquad (3)$$

where τ_{SMA} is the torque on the SMA wire, r is the lever linking the wire and the joint, ξ is the martensite fraction, E_A is elastic modulus of the austenite phase, A_t is the cross section area of the wire, l_0 is the undeformed length of the wire, l is the maximum length of the wire and x is the displacement of the wire. The martensite fraction depends on wire temperature and is given by the relation below (4):

$$\xi = \begin{cases} \dfrac{\xi_M}{1+e^{\left[\frac{6,2}{A_f - A_S}.\left(T - \frac{A_S + A_f}{2}\right)\right]}} & ;\ heating \\ \dfrac{1-\xi_A}{1+e^{\left[\frac{6,2}{M_S - M_f}.\left(T - \frac{M_S + M_f}{2}\right)\right]}} + \xi_A & ;\ cooling \end{cases} \qquad (4)$$

where ξ_M is the martensite fraction in the start of heating, A_s and A_f are the austenite temperatures at start and finish of phase transformation, and T is the wire temperature, ξ_A is the martensite fraction in the start of cooling M_s and M_f are the martensite temperatures at start and finish of phase transformation. Note that the phase transformation present hysteresis, therefore there is an equation to model the heating and another to model the cooling. The dynamics of wire temperature is given by (5):

$$m.c_p.\dot{T} = R.i^2 - h.A.(T - T_{amb}) \qquad (5)$$

where m, c_p, R and , A are, respectively, the mass, specific heat, ohmic resistance and heat exchange area of the wire. $\dot{T}$ is the temperature variation rate, i is the electrical current flowing through the wire, h is the convection coefficient and T_{amb} is the ambient temperature.

III. Impedance Controller Design

The control algorithm designed was based on previous results presented by Hogan [1] and Aguirre-Ollinger *et al.* [2, 3]. Its block diagram is illustrated next, in Fig. 2.

In order to modify the impedance perceived by the human user, the exoskeleton must apply adequate torques depending on both the angular position of the joint and the torque applied by the human. Thus, the controller receives as

input the torque measured between the human and the exoskeleton, $\tau_m = \tau_h - \tau_{exo}$. This signal goes through a block that implements the desired impedance transfer function (6), which is the impedance that the user should perceive when using the exoskeleton. Then, this block provides the position reference that can be fed to a PID controller that has a negative feedback from the plant (joint angle, θ) and gives a torque reference to the actuator. The actuator output, τ_{exo}, is summed to the human torque, τ_h. It must be noted that in this work the dynamics and control of the SMA actuator has been considered in the model. However, if another actuator was to be used, the only change needed would be the actuator block. It is also important to remark that the chosen actuator must have an embedded torque controller, given that the actuator block receives a desired torque as input and outputs the exoskeleton torque.

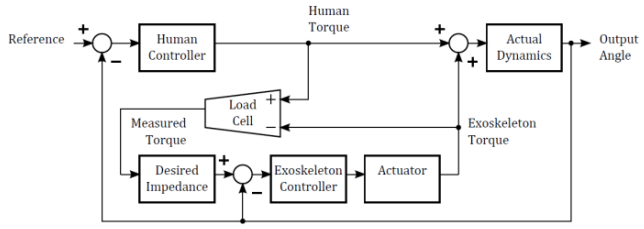

Fig. 2. Block diagram of the proposed impedance control algorithm. Both the Human Controller and the Exoskeleton Controller blocks were implemented using PID controllers. The Actuator block may be substituted by the control and dynamics of actuator used in each application.

The Actual Dynamics block contains the transfer function described in Eq. (2), i.e., the actual dynamics (human-exoskeleton); while the Desired Impedance block contains the following second-order transfer function (6):

$$\frac{\theta_d}{\tau_m} = \frac{1}{J_d.s^2 + B_d.s + K_d} \quad (6)$$

IV. SMA CONTROLLER DESIGN

To control the force of the SMA actuators, a two layer relay control based on results obtained by Grant and Hayward [12] was used. This controller has the advantage of simple implementation and robustness to variations in the plant model. Hence, the electrical current used to heat the wire could assume only two active values: 500 mA and 800 mA. The threshold value to change between both values was set to 0.1 N.m, i.e., when the error (reference torque given by the Exoskeleton Controller minus τ_{exo}) is lower than 0.1 N.m, the output is 500 mA; if higher, the output is 800 mA. As it will be showed next, such controller achieved satisfactory performance.

V. SIMULATION

The control scheme was implemented and simulated in MATLAB/Simulink (The MathWorks Inc., Natick, MA, USA). Human movement was simulated using chirp signals, as a means to evaluate the behavior of the impedance controller with increasing frequency (up to 2 Hz). The human controller was modeled as a PID. This simplification was used only to assess the human exoskeleton interaction. For a precise simulation of human behavior, a more detailed controller should be used, such as a pair of agonist-antagonist muscle models with reflex regulation [21].

A. Simulation of impedance control alone

The impedance controller was at first simulated without taking into account the actuator control and dynamics. The actuator was considered to be ideal, i.e., with unitary transfer function. In this way, the impedance control is generic and can be further modified to integrate any kind of actuator. Again, the only restriction in selecting the actuator is that it needs to be controlled by torque.

For this simulation, a Simulink model, similar to the block diagram depicted in Fig. 2, was used. Four cases were considered, as described next. In all of them, the input signal was a sinusoid with amplitude ranging from 0 to 40º and with increasing frequency from 0 to 2 Hz.

1) No assistance from the exoskeleton: in this case, the exoskeleton is not active and the human applies torque both to his leg and to the exoskeleton. Results are presented in Fig. 3. This serves as a reference result to evaluate the performance of the Human Controller.

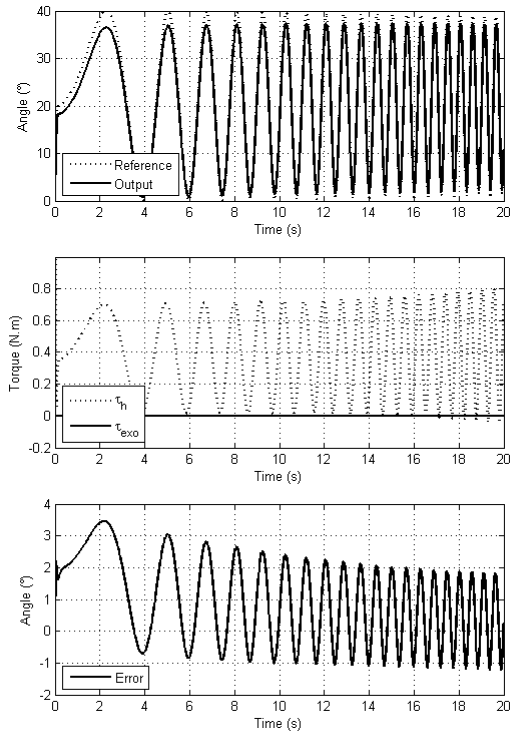

Fig. 3. Reference and output angle; torque applied by the human; and tracking error between reference and output angle versus time when the exoskeleton is not active.

2) Desired impedance lower than the actual impedance: in this case, the exoskeleton contributes to improve human performance. The desired impedance parameters used were: $J_d = J/4$, $B_d = B/4$, $K_d = K/4$. Results are presented in Fig. 4.

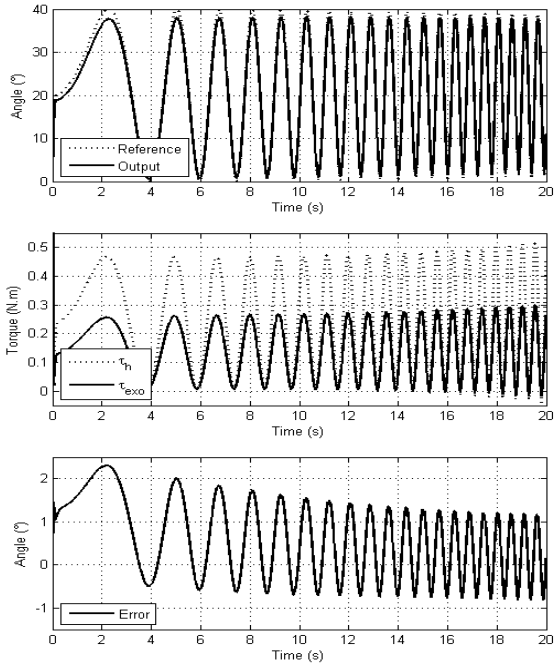

Fig. 4. Reference and output angles; torques applied by the human and the exoskeleton; and tracking error versus time when the exoskeleton is active and the desired impedance is lower than the actual impedance.

3) Desired impedance equal to human impedance: in this case, the human would experience no additional effort while using the exoskeleton. Therefore, the desired impedance parameters used were: $J_d = J_h$, $B_d = B_h$, $K_d = K_h$. Results are presented in Fig. 5.

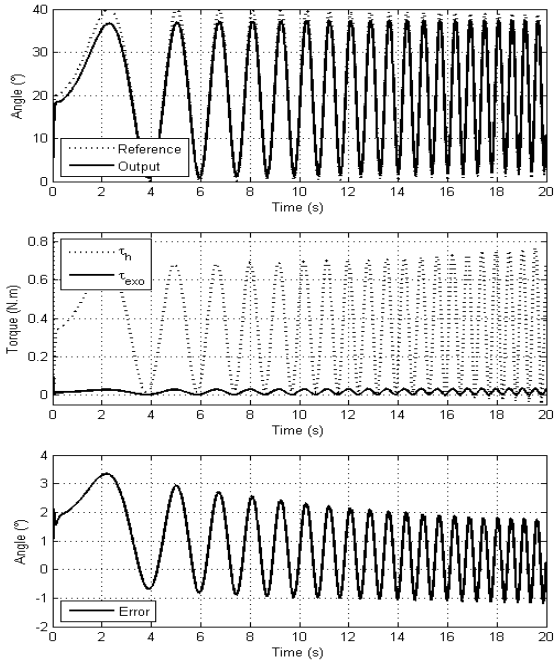

Fig. 5. Reference and output angles; torques applied by the human and the exoskeleton; and tracking error versus time when the exoskeleton is active and the desired impedance is equal to the human impedance.

4) Desired impedance higher than the actual impedance: in this last case, the exoskeleton actuates opposing the human effort. The desired impedance parameters used were: $J_d = 2.J$, $B_d = 2.B$ and $K_d = 2.K$. Results are presented in Fig. 6.

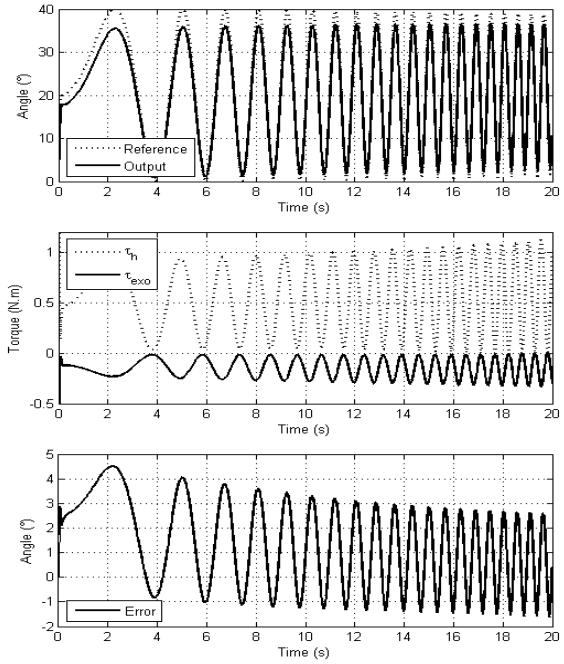

Fig. 6. Reference and output angles; torques applied by the human and the exoskeleton; and tracking error versus time when the exoskeleton is active and the desired impedance is higher than the actual impedance.

It must be noticed that in the four cases, the tracking error seems to be decreasing as frequency rises. In fact, the error increases if higher frequencies are considered. Tracking error for case *A.2*, with input frequency rising until 4Hz, is presented in Fig. 7.

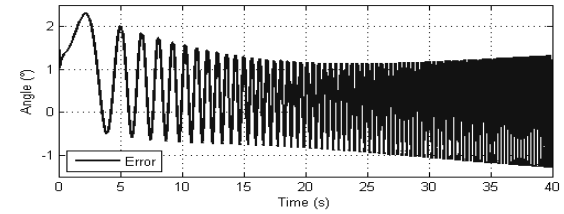

Fig. 7. Tracking error versus time when the exoskeleton is active and the desired impedance is lower than the actual impedance. Input frequency rises up to 4Hz.

B. Simulation of impedance control with SMA actuator

In this second scenario, the impedance control is simulated considering the SMA actuator dynamics and control (Actuator block). As mentioned, the proposed actuator cannot actuate in both negative and positive angular directions, so the case *A.4*, simulated before, is not feasible with this particular actuator. In this simulation, two cases were considered. Again, the input signal was sinusoidal ranging from 0 to 40º and with increasing frequency from 0 to 2 Hz. A third case, with a fixed frequency square wave input (1 Hz), was used to evaluate wide-band signal tracking performance of the SMA actuator.

1) Desired impedance lower than the actual impedance: in this case, the exoskeleton aids the human to improve his performance.

The desired impedance parameters used were $J_d = J/4$,

$B_d = B/4$ and $K_d = K/4$. Results are presented in Fig. 8.

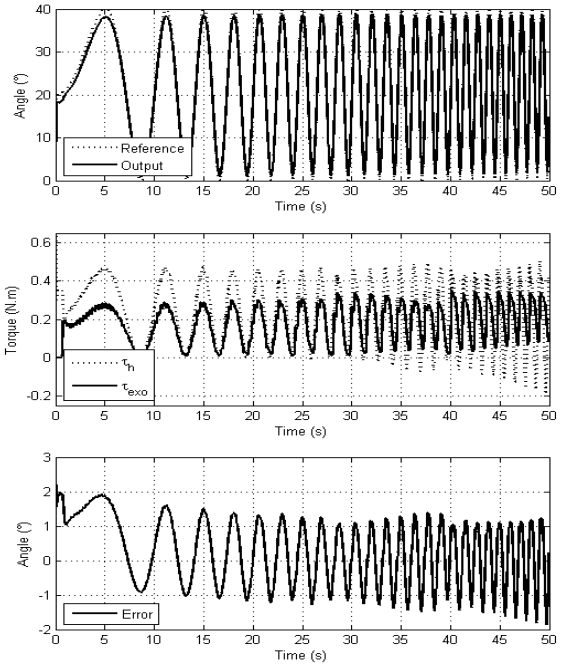

Fig. 8. Reference and output angles; torques applied by the human and the exoskeleton; and tracking error versus time when the exoskeleton is active and the desired impedance is lower than the actual impedance, considering the SMA actuator.

2) Desired impedance equal to human impedance: in this case, the human would experience no additional effort while using the exoskeleton. Thus, the desired impedance parameters used were: $J_d = J_h$, $B_d = B_h$ and $K_d = K_h$. Results are presented in Fig. 9.

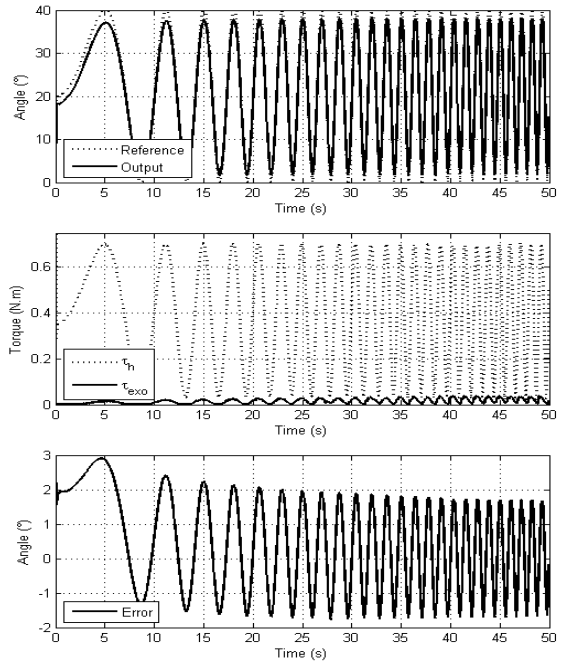

Fig. 9. Reference and output angles; torques applied by the human and the exoskeleton; and tracking error versus time when the exoskeleton is active and the desired impedance is equal to the human impedance, considering the SMA actuator.

3) Desired impedance equal to actual impedance and square wave input: this simulation was done to evaluate the controller performance to wide-band signal. Thus, a 1 Hz square wave reference signal was used. The desired impedance parameters used were $J_d = J/4$, $B_d = B/4$ and $K_d = K/4$. Notice that human actuation was limited to an absolute value of 1 N.m. Results are presented in Fig. 10.

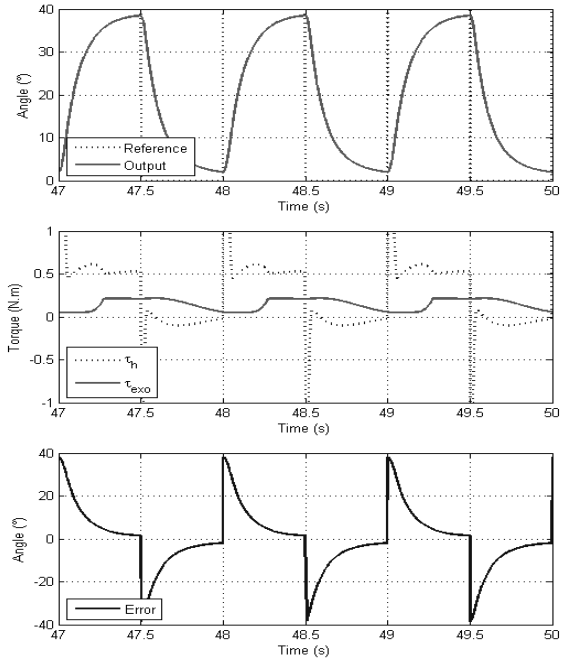

Fig. 10. Reference and output angles; torques applied by the human and the exoskeleton; and tracking error versus time when the exoskeleton is active and the desired impedance is lower than the actual impedance, considering the SMA actuator and wide-band input signal.

VI. Discussion

It is interesting to note that the PID controller used to simulate the human behavior acted cooperatively with the exoskeleton. It causes an increase in human torque to produce the movement against the exoskeleton when the desired impedance was larger than the actual, and, analogously, caused human torque reduction as the exoskeleton controller created a virtual impedance reduction. Another remarkable fact is that the tracking error decreases with the reduction of the desired impedance, as there is an increased intervention of the exoskeleton.

The introduction of the SMA dynamics worsened the performance of the impedance control. This actuator worked similar to the ideal actuator for frequencies until up to about 1 Hz, but for higher frequencies the response was limited by the cooling rate of the wires. The impedance controller, in conjunction with the SMA actuators, presented stable performance with wide-band signal input.

The preliminary simulation results presented in this work indicate the viability of the physical implementation of the proposed system and its controllers. However, there are still some topics which require further investigation:

1) A more realistic human controller: The PID controller used to simulate the human controller is too simplistic. Despite good interaction between Human Controller and Exoskeleton Controller blocks was achieved in this work, to

have a better idea of the human-exoskeleton interaction, a more precise human motor control model is needed.

2) An antagonistic actuator: If the exoskeleton presented an antagonistic actuator, then it could be also used to increase the impedance, as well as an improved frequency response. This kind of actuator could be implemented using two antagonist SMA wires or with one SMA actuating in one direction and a spring/damper to return the system to the equilibrium position. A force controlled antagonistic SMA actuator is being developed by Ianagui and Tannuri [22] which could be used to further improvement.

3) A more precise SMA controller: The two layer relay controller achieved acceptable tracking; nevertheless, this control algorithm introduced torque ripple, which could cause discomfort to the exoskeleton user. Romano and Tannuri [10] have developed a position control for SMA using Sliding Mode Control, which eliminates this undesired ripple. Such controller is under implementation in the proposed exoskeleton.

4) Prototype testing: A physical prototype is under development at University of São Paulo. Building and testing the reduced scale prototype is fundamental before definite conclusions about the viability of a full size exoskeleton are made.

5) SMA electrical drive and cooling: in human scale, several SMA wires are needed to achieve both the torque and frequency response requirements. The electric drive system might need to deliver powers in the order of tens of Watts per wire. Given the poor thermal efficiency of the wire (typically in the order of 1% [15]), if higher actuation bandwidth is demanded, active cooling must be used. A more detailed research is needed before estimating the human scale drive and cooling power requirements.

VII. CONCLUSION

The paper showed an overview of the proposed controller and preliminary simulation results. There is evidence that the system will work in real applications and results justified the construction of a physical prototype. However, because of the simplistic approach to simulate the controller, definitive conclusions cannot be made yet. Given that the proposed controller is generic, it will serve as a resource for future research on the control of various types of exoskeletons and others systems requiring impedance control.

VIII. ACKNOWLEGMENTS

Third author acknowledges the support from the Sao Paulo State Research Foundation - FAPESP (Brazil) grant 2010/17181-0). Second (E.A.T.) and third (A.F.C.) authors thank the National Research Council of Brazil CNPq for grants (302544/2010-0 to E.A.T.) and (308244/2009-5 and 478863/2010-1 to A.F.C).

REFERENCES

[1] N. Hogan, "Impedance control: an approach to manipulation," *Journal of Dynamic Systems, Measurement and Control*,.107, 1985, pp. 1-24.

[2] G. Aguirre-Ollinger, "Active impedance control of a lower limb assistive exoskeleton," Dissertation, Northwestern University, Evaston, USA, 2009.

[3] G. Aguirre-Ollinger, "A 1-DOF assistive exoskeleton with virtual negative damping: effects on the kinematic response of the lower limbs," *IEEE/RSJ International conference on intelligent robots and systems*, pp. 1938-1944, San Diego, USA, Dec. 2007.

[4] W. A. V. Valenzuela, A. M. N. Lima, J. S. Rocha Neto, "Robô bípede acionado com ligas de memória de forma," unpublished.

[5] K. Ikuta, M. Tsukamoto, S. Hirose, "Mathematical model and experimental verification of shape memory alloy for designing micro actuator," *IEEE Micro electro mechanical systems, an investigation of micro structures, sensors, actuators, machines and robots,* pp.103-108, Nara, Feb. 1991.

[6] H. M. Elahinia, H. Ashrafiuon, "Nonlinear control of a shape memory alloy actuated manipulator," *ASME Journal of Vibration and Acoustics*, vol. 124, pp 566-575, 2002.

[7] D. Grant, V. Hayward, A. Lu, "Design and comparison of high strain shape memory alloy actuators," *International conference on robotics and automation*, pp 260-265, Albuquerque, USA, 1997.

[8] S. M. Dutta, F. H. Ghorbel, "Differential hysteresis modeling of a shape memory alloy wire actuator," *IEEE/ASME Mechatronics*, vol. 10, pp. 189-197, Apr. 2005.

[9] K. Hoder, M. Vasina, F. Solc, "Shape memory alloy – unconventional actuators," *International conference on industrial technology*, pp. 190-193, Maribor, Slovenia, 2003.

[10] R. Romano, E. A. Tannuri, "Modeling, control and experimental validation of a novel actuator based on shape memory alloys," *Mechatronics (Oxford)*, v. 19, pp. 1169-1177, 2009.

[11] D. Grant, V. Hayward, "Design of shape memory alloy actuator with high strain and variable structure control," *IEEE International conference on robotics and automation*, vol. 3, pp. 2305-2312, Nagoya, Japan, 1995.

[12] D. Grant, V. Hayward, "Constrained force control of shape memory alloy actuators," *IEEE International conference on Robotics and automation*, vol.2, pp. 1314-1320, San Fransico, USA, 2000.

[13] F. Aral, D. Azuma, K. Narumi, Y. Yamanishi, Y.C. Lin, "Design and fabrication of a shape memory alloy actuated exoskeletal microarm," *International Symposium on Micro-NanoMechatronics and Human Science*, pp. 339-343, Nagoya, Japan, Nov. 2007.

[14] L. L. Ammar, B. Y. Kaddouh, M. K. Mohanna, I. H. Elhajj, "SAS: SMA Aiding Sleeve," *IEEE International conference on robotics and biomimetics*, pp. 1596-1599, Tianjin, China, Dec. 2010.

[15] P. P. Abolfathi, "Development of an instrumented and powered exoskeleton for the rehabilitation of the hand," Thesis presented for the degree of Doctor of Philosophy, School of Aerospace, Mechanical and Mechatronic Engineering, University of Sydney, 2007.

[16] J. Colorado, A. Barrientos, C. Rossi, "Músculos inteligentes en robots biológicamente inspirados: modelado, control y actuación," *Revista iberoamericana de automática e informática industrial*, vol. 08, pp. 385-396, 2011.

[17] J. Urata, T. Yoshikai, I. Mizuushi, M. Inaba, "Design of high D.O.F. mobile micro robot using electrical resistance control of shape memory alloy," *IEEE/RSJ International conference on intelligent robots and systems*, pp. 3828-3833, San Diego, USA, Dec. 2007.

[18] M. Nishida, K. Tanaka, H. Q. Wang, "Development and control of a micro biped walking robot using shape memory alloys," *IEEE Conference on robotics and automation*, pp. 1604-1609, Mar. 2006.

[19] M. Terauchi, K. Zenba, A. Shimada, M. Fujita, "Controller design on the fingerspelling robot hand using shape memory alloy," *International joint conference SICE-ICASE*, pp. 3480-3483, 2006.

[20] H. P. Crowell III, A. C. Boynton, M. Mungiole, "Exoskeleton power and torque requirements based on human biomechanics," Army Researh Laboratory, Technical Report ARL-TR-2764, 2002.

[21] N. Lan, Y. Li, Y. Sun, F. S. Yang, "Reflex regulation of antagonist muscles for control of joint equilibrium position," *IEEE Trans. Neural systems and rehabilitation engineering*, vol. 13, pp. 60-71, Mar. 2005.

[22] A. S. S. Ianagui, E. A. Tannuri, "Modeling and control of an antagonistic shape memory allow actuator," *21st Brazilian Congress of Mechanical Engineering*, Natal, Brazil, 2011.